Biomass and Bioenergy 181 (2024) 107056

Contents lists available at ScienceDirect

Biomass and Bioenergy

journal homepage: www.elsevier.com/locate/biombioe

Oligomeric fragments distribution, structure and functionalities upon ruthenium-catalyzed technical lignin depolymerization

Tina Ročnik Kozmelj [a,b], Erika Bartolomei [c], Anthony Dufour [c], Sebastien Leclerc [c], Philippe Arnoux [c], Blaž Likozar [a], Edita Jasiukaitytė-Grojzdek [a,*], Miha Grilc [a,b], Yann Le Brech [c,**]

[a] Department of Catalysis and Chemical Reaction Engineering, National Institute of Chemistry, Hajdrihova 19, 1001, Ljubljana, Slovenia
[b] University of Nova Gorica, Vipavska 13, 5000 Nova Gorica, Slovenia
[c] University of Lorraine, LRGP, CNRS, 1 rue Grandville, 54000, Nancy, France

ARTICLE INFO

Keywords:
Condensation
Depolymerization
NMR spectroscopy
Oligomers
Ruthenium
Technical lignin

ABSTRACT

The development of effective lignin depolymerization is essential for the extraction of aromatic building blocks from renewable resources. In this study, technical lignins (Soda and Kraft) were depolymerized in supercritical ethanol using Ru/C as a catalyst in an inert (N_2) or a reducing (H_2) atmosphere. The effects of lignin structure and atmosphere were studied on the depolymerization, and the products formed such as solid residue, oligomeric fragments and monomers. Reasonable yields of oligomers and monomers (32.7 wt% and 4.7 wt%, respectively) were obtained after Ru/C-assisted Soda lignin depolymerization under both tested atmospheres, while in the case of Kraft lignin, H_2 and Ru/C were required to increase the yields of depolymerization products (30.9 wt% and 4.4 wt%, respectively). A comprehensive characterization of the reaction products (GC-MS, UV fluorescence and FTIR spectroscopy, ^{31}P and 2D HSQC NMR) was performed to evaluate the monomer/oligomer distribution and to determine the structure and functionalities of the oligomers. The analytical results indicate the formation of more condensed oligomeric lignin structures with predominant 5-5′ inter-unit linkages and the prevalence of demethylation or demethoxylation reactions depending on the type of the technical lignin exposed to hydrodeoxygenation. The oligomeric fragments are catalytically modified and depolymerized lignin with a wide range of new applications (coatings, resins, antioxidant agents, adhesives) contributing to the replacement of the petroleum-derived phenolic building-blocks.

1. Introduction

One of the main goals in the last decade is to be able to replace fossil fuel resources and produce greener and sustainable energy, fuels and chemicals from renewable resources. Lignin is described as natural aromatic resource for potential production of bio-derived fuels, various chemicals or precursors for polymer synthesis [1–4]. Pulp and paper industries are the main industrial source of lignin. Despites the abundant number of research focusing on lignin conversion into high-value products [2,5], currently, most of the lignin produced from pulp industries is burned to generate electricity and heat [6]. Indeed, lignin production is estimated to be 50–70 million tons annually [7]. Therefore, lignin is one of the most abundant renewable materials. Its valorization is one of the most promising ways for the substitution of fossil resources to produce aromatic compounds. However, technical lignins from pulp industries (mostly Soda and Kraft lignins) present condensed structures making their valorization and depolymerization difficult [8]. In order to tackle this structural features, different methodologies have been applied to convert lignin to high-value compounds [9–12].

In the native biomass, lignin consists of a three-dimensional aromatic polymer composed of phenylpropenyl units, which are randomly connected through carbon-carbon (C-C) and carbon-oxygen (C-O) (ether) bonds [5,13]. The ether linkages abundance in native lignin is relatively high (45–48 %) and the repartition between different linkages is function of the biomass type (softwood, hardwood, herbaceous) [14]. During the pulping process of woody biomass, most of the ether linkages are cleaved [15,16]. Indeed, the β-O-4 and α-O-4 linkages are cleaved leading to the formation of C-C linkages by condensation reactions

* Corresponding author.
** Corresponding author.
E-mail addresses: edita.jasiukaityte@ki.si (E. Jasiukaitytė-Grojzdek), yann.le-brech@univ-lorraine.fr (Y. Le Brech).

https://doi.org/10.1016/j.biombioe.2024.107056
Received 17 February 2023; Received in revised form 12 December 2023; Accepted 10 January 2024
Available online 18 January 2024

whereas natural C-C linkages are mostly preserved [2,5]. According to these structural modifications, lignin structure is dramatically changed and technical lignins are described as highly condensed aromatic structures where the low β–ether bonds need to be considered for lignin valorization strategies [17,18].

In order to develop an effective technology that converts lignin to fuel or marketable chemicals, one challenge is to depolymerize technical lignins to phenolic monomers or oligomers (partly depolymerized lignin). Reductive depolymerization with supported metal catalyst and molecular hydrogen (H_2) is one of the approaches widely studied [19]. Noble metal catalysts (Pt, Pd and Ru) still attract interest due to their high performance in reductive conditions for effective lignin hydrogenolysis [19–22] and char formation suppression [23,24]. Liquid-phase mild hydroprocessing (<300 °C and <10 MPa H_2 r. t) enable the preservation of methoxy groups with a high selectivity to alkyl-methoxyphenol products [2]. Alcohol solvents (methanol, ethanol, *iso*-propanol, etc.) have been used because of their capacity to dissolve lignin and its depolymerized products, their hydrogen-donor abilities, high heat transfer and dispersion capacity [20,24]. Ethanol is preferred as a solvent for lignin depolymerization as it improves the sustainability and profitability of a second-generation biorefinery [25], and its use has even been reported to result in higher monomer yields compared to methanol or *iso*-propanol [26,27]. The role of ethanol is to stabilize active intermediates and monomers, while serving as a radical scavenger to suppress condensation reactions. However, the role of ethanol is enhanced by the external hydrogen supply, which generates active hydrogen atoms over the catalyst to avoid condensation [26]. On the other hand, supercritical ethanol conditions were selected based on the improved solvent properties, technical lignin solubility, temperature activation of the solid catalyst and the lower activation barrier for bond cleavage [28,29].

Ru/C accelerates the C-O bond cleavage in the β-O-4 moiety and stabilize reactive radicals to avoid condensation to recalcitrant products even at mild reaction conditions [30,31]. To the best of our knowledge, the effect of the different lignin structure and catalysts (noble or transition metal catalysts on different supports) has been studied under mild reaction conditions [32–34]. However, the effect of the atmosphere (H_2 or N_2) on lignin depolymerization products is still poorly understood and notably under supercritical ethanol.

Technical lignins are limited by their low content of easily cleavable bonds, which is due to the harsh isolation process. Nevertheless, there is an opportunity to valorize technical lignin to produce valuable products, not only lignin monomers, but also oligomeric lignin fragments, which in combination with a tailored downstream process, have a tremendous potential to replace the petroleum-derived phenolic building-blocks. Oligomeric fragments are catalytically modified and depolymerized lignin with a modified chemical structure. The modification is beneficial for several valuable applications, e.g. high-performance adhesives, as antioxidant agents with improved antioxidant capacity, nanomaterials, films and coatings [35–39].

In this work, we investigate the influence of an inert (N_2) and a reductive (H_2) atmosphere on lignin depolymerization (LD) and product distribution of two technical lignins (Soda and Kraft) under mild reaction conditions (250 °C, 11.5 MPa) in supercritical ethanol. This work has a special focus on the effect of H_2/N_2 on products composition and highlights the chemical structure of oligomeric fragments with nuclear magnetic resonance (NMR) analysis. The lignins structure was characterized by several analytical techniques (elemental analysis, gel permeation chromatography, Fluorescence and FTIR spectroscopy, and nuclear magnetic resonance) to compare and investigate the effect of atmosphere on the structure of products after catalytic and non-catalytic process. To the best of our knowledge, this study is the first one to elucidate in detail the effect of H_2 during technical lignins conversion in supercritical ethanol with a special emphasis on the chemical structure of oligomers (^{31}P and 2D HSQC NMR).

2. Experimental section

2.1. Lignins and chemicals

Protobind 1000 lignin produced by soda pulping of wheat straw was supplied by GreenValue® (Schwaig, Nürnberg, Germany). Kraft lignin was produced from pinewood [33] by Centre Technique du Papier (CTP, Grenoble, France). The lignins, catalyst, solvent, chemicals and gases were used without further purification. The purity, suppliers and reference numbers of chemicals are provided in Supporting Information.

2.2. Lignin depolymerization experiment

The experiments were performed in a 300 mL autoclave Parr Instrument (Series 4890, Moline, IL, USA). The reactor was filled with 10 g of lignin, 200 mL of pure ethanol and 100 μL of hexadecane as internal standard to quantify monophenols by GC-MS. For catalytic test, 2.0 g of solid Ru/C catalyst (5 wt% Ru loading) was added to reach 1 wt% Ru on lignin. After sealing, the reactor was purged 3 times with nitrogen and subsequently charged (1 MPa) with nitrogen or hydrogen when reductive atmosphere was applied. The autoclave was heated up to 250 °C (~5 K min^{-1}) and hold at 250 °C (total pressure reached 11.5 MPa) for 4 h under continuous stirring at 1000 min^{-1}. The time 0 h referred to the time when the final temperature was reached. During the experiment, samples (3 mL) were collected every 30 min through a sampling line directly from the autoclave. Samples were filtered with 0.45 μm filters before further analysis. After the 4 h at isothermal condition, the reactor was cooled with compressed air flushing the outer surface of the reactor. The autoclave content was washed with ethanol to final 300 mL volume of ethanol solution with LD products. The entire mixture was filtered on a glass filter (11 μm). The filtrated fraction was not soluble in ethanol and after drying for 24 h at room temperature represented the "solid residue" (SR). The mass of SR includes the mass of char formed during LD. The mass of catalyst (if used) was excluded from the SR mass, so the catalyst mass has no effect on the reported solid residue yield. The final mass of SR was calculated by Eq. (1).

$$Solid\ residue\ (wt\%) = \left(\frac{m_{solid} - m_{catalyst}}{m_{lignin}}\right) \times 100 \qquad \text{Eq. (1)}$$

where m_{solid} stands for the mass of SR generated during the LD, while m_{lignin} represents the dry mass of lignin.

An acidification of the ethanol soluble products was performed by adding water and hydrochloric acid following the method proposed by Huang et al. [40] and filtrated through two filters (11 μm and 1.2 μm). The filter cake after acidic precipitation and vacuum drying at 40 °C was represented as lignin oligomers and the mass was calculated by Eq. (2).

$$Oligomers\ (wt\%) = \left(\frac{m_{oligomer}}{m_{lignin}}\right) \times 100 \qquad \text{Eq. (2)}$$

where $m_{oligomer}$ represents the mass in precipitated solid products after acidification and m_{lignin} is the lignin dry mass.

All the experiments performed are summarized in Table S1.

2.3. Elemental analysis

The oxygen weight percentages of the precipitated oligomers were determined using an elemental analyzer ThermoFisher Flash EA111 (Thermo Fisher Scientific, Waltham, MA, USA) in pyrolysis mode (Helium, 1100 °C). Carbon, hydrogen, nitrogen and sulphur contents were detected as gaseous products (carbon dioxide, water vapor, nitrogen, sulphur dioxide) after combustion at 1000 °C by oxygen injection to helium atmosphere. Elemental analysis was used for initial Soda and Kraft lignin, as well for the oligomers obtained after each experiment.

2.4. GPC analysis

Prominence HPLC system (Shimadzu, Kyoto, Japan) was used to determine the molecular weight distribution of the LD products. The precipitated oligomers and filtrated final liquid samples from the reaction were diluted in tetrahydrofuran (THF, 25 v/v% of sample), the same solvent of the mobile phase used for gel permeation chromatography (GPC). The detailed protocol was explained in detail in previous published work [33,41].

2.5. UV fluorescence: degree of depolymerization

UV fluorescence spectroscopy was applied to quantify soluble lignin fragments. UV fluorescence procedure was described in detail in previous work [41]. Curve-deconvolution was performed for interpretation of the UV spectra using Origin software (Originlab, Northampton, MA, USA) following the methods reported by Bartolomei et al. [41] Based on this previous work, depolymerization index (DI) can be calculated by Eq. (3) and monomeric product index (MPI) by Eq. (4),

$$DI = \frac{A_{306} + A_{350}}{A_{306} + A_{350} + A_{375}} \quad \text{Eq. (3)}$$

$$MPI = \frac{A_{306}}{A_{306} + A_{350} + A_{375}} \quad \text{Eq. (4)}$$

where A_{306} is the area of the deconvoluted peak at 306 nm, A_{350} at 350 nm and A_{375} at 375 nm. UV fluorescence analysis was carried out for the final liquid samples after 4 h of LD.

2.6. FTIR analysis

Fourier-transform infrared (FTIR) spectroscopy was acquired using FTIR ATR Bruker Alpha P spectrometer (Ettlingen, Germany). The method was used for both technical lignins and oligomers where ATR spectra were collected with 4 cm^{-1} resolution and the results were averaged of 64 scans with manual baseline correction and normalization.

2.7. 2D HSQC and ^{31}P NMR analysis

2D heteronuclear single quantum coherence (HSQC) NMR spectra of lignins and oligomers were recorded on a Bruker AVANCE NEO 600 MHz spectrometer equipped with BBFO probe following the reported protocol in previous published works [41,42]. Approximately 85 mg of lignin or oligomeric sample was dissolved in 0.60 mL of DMSO-d_6, which was used as an internal reference point (δ_C 39.5; δ_H 2.50 ppm). HSQC spectra analysis, calculations and assignation of lignin cross-signals were formulated following the published procedure [43].

Quantitative ^{31}P NMR experiments were performed following the protocol reported elsewhere [44,45]. Lignin and oligomer samples were derivatized using 2-chloro-4,4,5,5-tetramethyl-1,2,3-dioxaphospholane (TMDP) while the measurements were carried out in $CDCl_3$/pyridine 1:1.6 mixture with *N*-hydroxy-5-norbornene-2,3-dicarboxylic acid imide (NHND) as an internal standard.

2.8. GC-MS: detection of monomeric components

The samples without additional dilution were analyzed by an Agilent 7890 gas chromatograph (GC) coupled with Agilent 5975C mass spectrometer (MS) and flame ionization detector (FID) placed in parallel to the MS, equipped with an Agilent HP–5MS (5 % phenyl, 95 % methyl siloxane) column (Santa Clara, CA, USA). The NIST database was applied to identify more than 40 compounds by comparison of the mass spectra with the library. The quantification was based on the internal standard using the FID detector by following the de Saint Laumer's method which gives a prediction of the relative response factor [46,47].

3. Results

3.1. Lignin composition and characterization

As lignin structure and elemental composition is dependent on the source of biomass and its pretreatment method, Soda and Kraft lignin was characterized using elemental analysis, GPC and 2D NMR (Table 1 and Table S2). The elemental composition, molecular weight and the content of the most common linkages (β-O-4, β-5, β-β) in technical lignins are in accordance with published literature [48–50]. Intensive cross signals corresponding to the guaiacyl (G) and syringyl (S) units were observed at δ_C 108.5–122; δ_H 6.46–7.20 ppm and δ_C 102–108; δ_H 6.28–7.30 ppm, respectively, giving the S/G of 2.1 for Soda and 0.01 for Kraft lignin. The content of β-O-4, β-5 and β-β bonds was determined to be 3.5, 0.8 and 3.4 per 100C9 units for Soda lignin, and slightly higher contents of 8.1, 2.0 and 5.3 per 100C9 units for Kraft lignin, respectively. Moreover, the molecular weight for Soda and Kraft lignin was 4200 and 8600 g mol^{-1}, respectively.

3.2. Recovery product yields

The yields of the recovered products (solid residue, oligomers, monomers) after different reaction conditions are shown in Fig. 1 for Soda and Kraft lignin while the reproducibility of lignin depolymerization is presented in Fig. S1. The unrecovered products may be non-analyzed gaseous phase, unprecipitated oligomers and non-detected monomers by GC-MS. In general, the gasses present in the gaseous phase are CO_2, CH_4, H_2O and H_2S in the case of kraft lignin [51], while some hydrocarbons could be produced by solvent gasification [13]. For both lignins, experiments under inert atmosphere (N_2) and without catalyst showed the formation of high amount of SR, about 40.9 wt% for Soda and 50.1 wt% for Kraft lignin which is consistent with previous studies presenting close reaction conditions [19,24,40]. In non-catalytic trials, the insoluble residue is a result of the char-forming reactions. The char formation occurs by the condensation of the oligomers. Lignin depolymerization products such as phenolic oligomers and monomers were reported to be highly reactive [24,31]. Ether-bonds in lignin are cleaved and lead to the formation of free reactive phenolic hydroxyl groups [52] (through radical or charged species) and unsaturated side chains which are further involved in condensation reactions [40,53]. By adding the reductive atmosphere (H_2), the amount of SR was reduced from 40.9 wt% to 36.7 wt% in the case of Soda lignin and from 50.1 wt% to 40.7 wt% in the case of Kraft lignin. The presence of catalyst (Ru/C) additionally impedes the char-forming reactions thus reducing the amount of SR after the treatment for both Kraft and Soda lignin to 21.4 wt% and 12.3 wt% under H_2, and to 28.1 wt% and 16.3 wt% under N_2, respectively.

A significant evolution is observed in the yields of recovered oligomers. During the non-catalytic Kraft lignin depolymerization, the oligomer yield increases from 11.5 wt% (N_2) to 17.4 wt% (H_2) whereas it increases from 12.8 wt% (N_2) to 16.9 wt% (H_2) for Soda lignin. Consequently, H_2 appears to act to stabilize lignin oligomeric fragments during LD without a catalyst. Furthermore, Ru/C-catalyzed reactions additionally increased the oligomers content under inert and reductive atmosphere. As it is evident in Fig. 1, Soda lignin was more readily

Table 1
Average molecular weight, dispersity and the content of major structures in Soda and Kraft lignin.

Lignin	GPC		2D HSQC (per 100C9 units)			
	Mw (Da)	Dispersity	β-O-4	β-5	β-β	S/G
Soda	4200	1.50	3.5	0.8	3.4	2.1
Kraft	8600	1.84	8.1	2.0	5.3	0.01

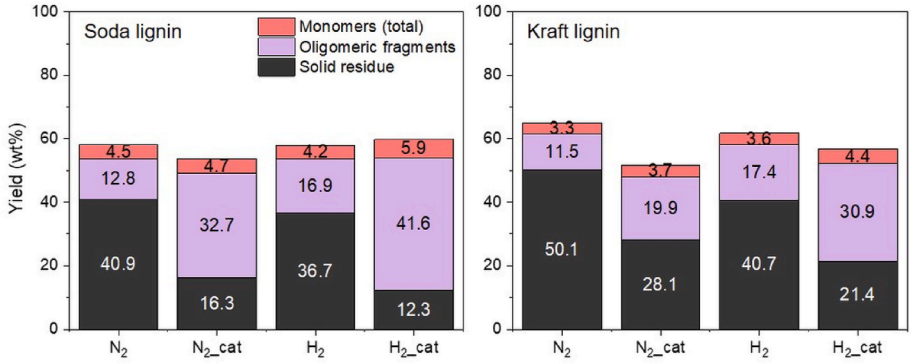

Fig. 1. Yields of the products at different reaction conditions.

converted into oligomeric fragments in Ru/C-catalyzed reactions under N_2 and H_2 atmospheres with yields of 32.7 wt% and 41.6 wt%, respectively. Kraft lignin catalytic depolymerization produced 19.9 wt% and 30.9 wt% of oligomers under N_2 and H_2, correspondingly. Though, a higher increase in the amount of oligomeric fragments was observed with Kraft lignin compared to Soda lignin for catalytic depolymerization under N_2 and H_2. Therefore, the effect of H_2 is more beneficial to Kraft lignin and a Ru/C catalyst is required to promote efficient lignin depolymerization [33,54].

The amount of monomers was evaluated by GC-MS analysis. The highest yields of monomers were achieved after the catalytic hydrogenation of both technical lignins which made 5.9 wt% and 4.4 wt% in case of Soda lignin and Kraft lignin, respectively. Despite the different treatment conditions applied, only a minor difference between the monomer yields was observed implying that in both cases, lignin macromolecule was more likely converted into the oligomeric fragments rather than into the monomers. Analogous lignin behavior under the reductive conditions has been reported by Long et al. [55]. On the other hand, the monomer yield after depolymerization of technical lignin compared to lignins structurally close to native lignin is not significant, but the reported theoretical monomer yield for technical lignin (soda and kraft) was less than 4 % when only the easily cleavable bonds are considered [56]. From this we can conclude that we obtained monomer yields that are close to the theoretical values for technical lignins.

3.3. Elemental analysis of oligomers

Elemental composition of lignin oligomers is presented in Van Krevelen diagrams describing atomic ratio between carbon, oxygen and hydrogen for each reaction condition (Fig. 2). Detailed results concerning weight percentages (C, H, O, N, S) and total atomic balances are presented in Table S2.

The atomic ratios for Soda, Kraft lignins and oligomers are consistent with the literature [40,48,49]. The ranges of H/C and O/C that are expected for lignin and lignin oligomers are approximately 0.8–1.3 and 0.2–0.5, respectively [57]. Generally, the decrease of the O/C atomic ratio in oligomers is observed for each condition compared to lignin whereas H/C ratio increases (Fig. 2). This can be explained by the hydrogenolysis of C-O bonds, hydrogenation of functional groups and unsaturated propyl chains during LD. The O/C decrease is more significant in experiments with Soda than with Kraft lignin due to the higher O/C ratio in the starting Soda lignin and hydrodeoxygenation of syringyl units and carboxylic acids. The change in elemental composition is attributed to the Ru-catalyst activity and the external hydrogen source, while ethanol served as H-donor for the hydrogenation under a nitrogen atmosphere. Furthermore, the carbon content in oligomers could increase compared to the initial lignin due to rearrangements and C-C bond formation (condensation) within the depolymerized products – oligomers.

3.4. GPC analysis of lignin oil and precipitated oligomers

GPC was used for filtrated lignin oil obtained after LD and for precipitated oligomers. The Mw of lignin liquid samples after depolymerization was between 650 and 770 Da for all reaction conditions and the results are presented in Table S3. The mass average molecular weight (Mw) values are slightly higher for catalytic LD which is in line with higher amount of precipitated oligomers contained in lignin oil. This observation is in agreement with previous studies [20,23,24]. Although, the lignin oils could contain monomers, dimers, trimers, etc., the separation was not achieved since the used column and method exhibit single peak with a unimodal distribution.

Furthermore, Mw of precipitated oligomers was around 1050 Da (Table S3) for each reaction condition meaning that the molecular weight of oligomers is considerably lower in comparison to initial technical lignins (Table 1). Therefore, lignin macromolecule was

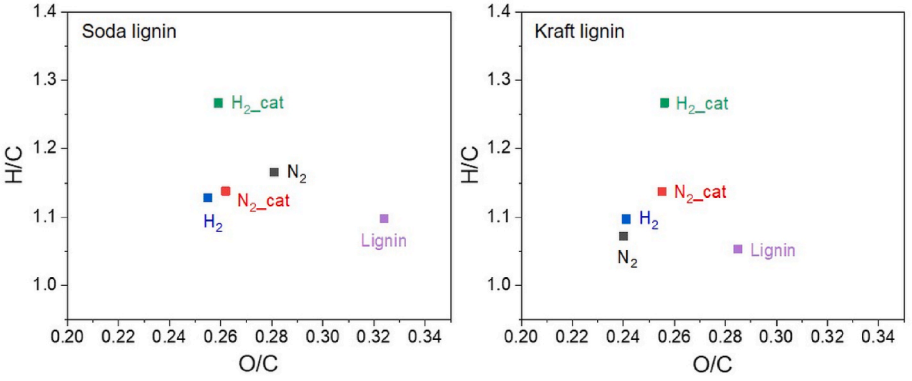

Fig. 2. Van Krevelen diagram of lignins and precipitated oligomers.

depolymerized to smaller, however more condensed fragments were formed under inert and reductive atmosphere.

3.5. UV fluorescence

UV synchronous fluorescence spectra have shown important different peak maxima and intensities depending mainly on the type of molecule [41]. According to LD products, three main peaks (Fig. S3) are observed on the emission spectra. These peaks were assigned based on the analysis of model compounds [41]. The emission peak at 306 nm is assigned to monomers fluorescence, while oligomers emission peak is established around 350 nm. The third peak at 375 nm is dedicated to dissolved lignin or heavy aromatic condensed components soluble in ethanol. This method has been used to compare the efficiency of all the experiments and to evaluate the effect of the reaction conditions on the extent of LD. The semi-quantitative indexes as DI and MPI were defined to describe the relative distribution between depolymerized components (oligomers and monomers) and relative distribution of detected monomers, respectively. The index values are presented in Table S4.

The DI (oligomers and monomers) and MPI (monomers) increase with the reaction time for both tested lignins though with different trends (Fig. 3). Interestingly, the evolution of DI value is similar for catalytic and non-catalytic reaction under inert and reductive atmosphere for Soda lignin. An important increase of DI value is observed between 2 h and 4 h of reaction time with the maximum at 0.76 for Soda catalytic LD. Moreover, the high MPI is observed only for catalytic and reductive condition with the maximum at 0.32 while other conditions ineffectively promote formation of monomeric components (Fig. 3). Differently to Soda lignin, DI barely increased during time and different reaction conditions for Kraft lignin except for H_2_cat experiment where DI increase up to 0.89 after 4 h of conversion. The DI and MPI are relatively low under inert and non-catalytic reactions at the final reaction time for the Kraft lignin. A high MPI for Kraft lignin was detected only for catalytic and reductive LD (H_2_cat) with maximum at 0.29 and it is comparable to Soda lignin under the same conditions (catalyst and H_2).

3.6. NMR analysis

While FTIR analysis (Fig. S3) was used to distinguish characteristic monolignols and linkages in lignin and its oligomers, a comprehensive 2D HSQC and quantitative ^{31}P NMR analysis were applied to provide detailed structural information of initial technical lignins and precipitated oligomers [58] of the best performing experiment (H_2_cat), specifically to quantify changes within the G-, S-units and C-O, C-C linkages. The results of 2D HSQC analysis are presented in Fig. 4 and the table with ^{1}H-^{13}C chemical shifts is added to Supporting Information (Table S5). As expected, the structural features of Soda and Kraft lignin depend on biomass source, which is mainly reflected in the S/G ratio. The measured S/G/H ratio in Soda lignin is 67/31/2 which exhibits a low contribution in *p*-hydroxyphenyl (H) units. The emergence of the syringyl neighboring to OH at Cα (S) and syringyl neighboring carbonyl group (S′) in Soda lignin/oligomeric fragments is clearly shown by the intensive cross signals at δ_C 102–104; δ_H 6.65–6.95 ppm and δ_C 104–107; δ_H 6.25–6.75 ppm, respectively. Moreover, Soda and Kraft lignin appear as three guaiacyl-based contours indicated with the cross signals at δ_C 108.5–111.5; δ_H 6.78–7.14 ppm, δ_C 112.5–114; δ_H 6.48–7.06 ppm and δ_C 115–118; δ_H 6.65–6.96 ppm corresponding to the G_2, G_5 and condensed guaiacyls, and G_6, respectively. In spectra of obtained oligomers, a partial shift of the cross signal corresponding to G_2 and G_6 from δ_C 108–111.5; δ_H 6.78–7.14 ppm to δ_C 107–109; δ_H 6.55–7.45 ppm and δ_C 115–118; δ_H 6.65–6.96 ppm to δ_C 117–122; δ_H 6.4–6.75 ppm, respectively, reveals the formation of 5-5′ interunit linkage as a result of G-units condensation [59]. Indeed, an analogous shift of the G_2 and G_6 cross-signal due to coupling within the G-units was confirmed with the model compound *3,3′-dimethoxy-1,1′ dimethyl biphenyl* and during kraft pulping by Giummarella et al. [59]. Furthermore, Lancefield et al. [60] synthesized and analyzed advanced lignin model polymers to confirm and demonstrate the abundance of inter-unit linkages (e.g., β-O-4, β-5 and β-β) in lignin. Additionally, there is a clear tendency for condensed structures within the S units to be preserved in Soda lignin oligomers.

The β-O-4 bond (A) cleavage was confirmed by disappearance of the cross signal at δ_C 71–74 and δ_H 4.7–5.0 ppm. On the other hand, the

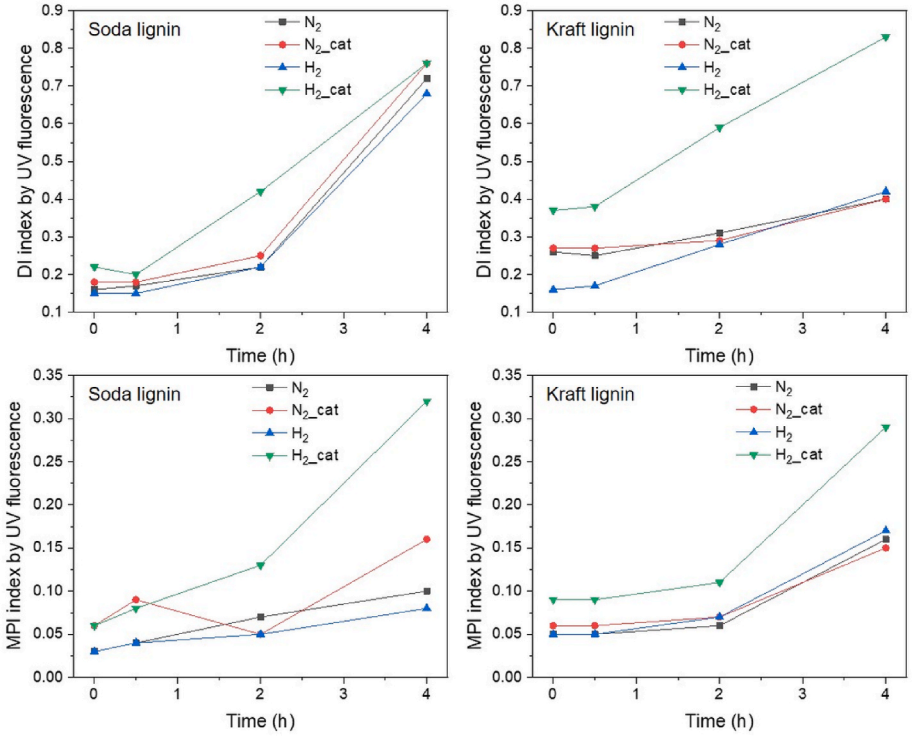

Fig. 3. Relative distribution indexes (DI and MPI) for technical lignins depolymerization as function of reaction time.

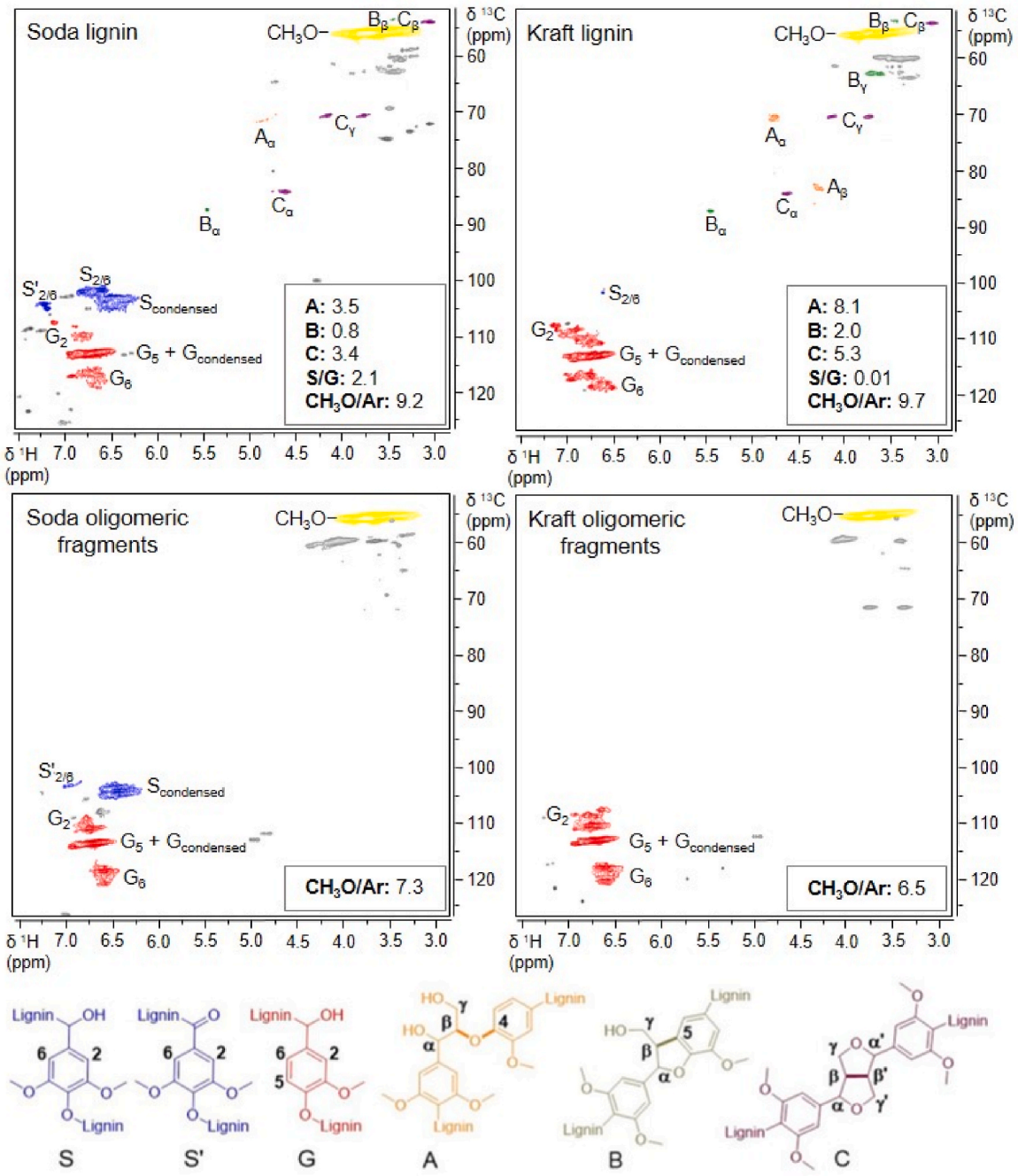

Fig. 4. Comparison of the 2D HSQC NMR spectra of Soda and Kraft lignin and its oligomeric fragments following catalytic reaction at 250 °C for 4 h with the Ru/C catalyst (H_2). The amounts of the major linkages are calculated per 100C9 units [43].

scarcity of β-5 (B) and β-β (C) substructures have been noticed in the analyzed oligomeric fragments, indicating a remarkable reduction in lignin complexity, rearrangements within its structure and decrease in molecular weight.

The main findings revealed by 2D HSQC NMR are summarized in Fig. 5. The highlight of LD is that the β-O-4 bond cleavage generated more guaiacyl rich dimeric/oligomeric fragments which further formed condensed oligomeric structures creating new 5-5′ interunit linkages. Crestini et al. [8] and Gierer et al. [61] similarly described a highly condensed structures by direct radical coupling of aromatic rings. On the other hand, ^{31}P NMR studies on softwood (kraft) lignin support the proposed radical coupling within aromatic rings, as Granata et al. [62] described a division of C_5-substituents into three regions: 5-5′ substructures (140–142 ppm), coupling within aromatic rings by oxygen bridge (142–143 ppm) and β-5 substructures (143–144 ppm). Fig. S4 and Table S6 show a higher content of C_5-substituted hydroxyl groups supporting the formation of condensed 5-substituted units through either by 5-5' or β-5 coupling, which is typically only for lignin with guaiacyl units [44,63].

Quantitative ^{31}P NMR analysis was performed to assess the different OH groups in lignin samples [44]. Thus the change of the phenolic and aliphatic OH group content was determined at different reaction conditions and summarized in Fig. 6. The phenolic OH group content represents a total amount of the C_5-substituted (including syringyl OH groups for Soda lignin) guaiacyl and *p*-hydroxyphenyl OH groups (Table S6).

The total OH group content was determined to be 4.6 mmol g^{-1} and 5.7 mmol g^{-1} in Soda and Kraft lignin, respectively. The ^{31}P NMR results

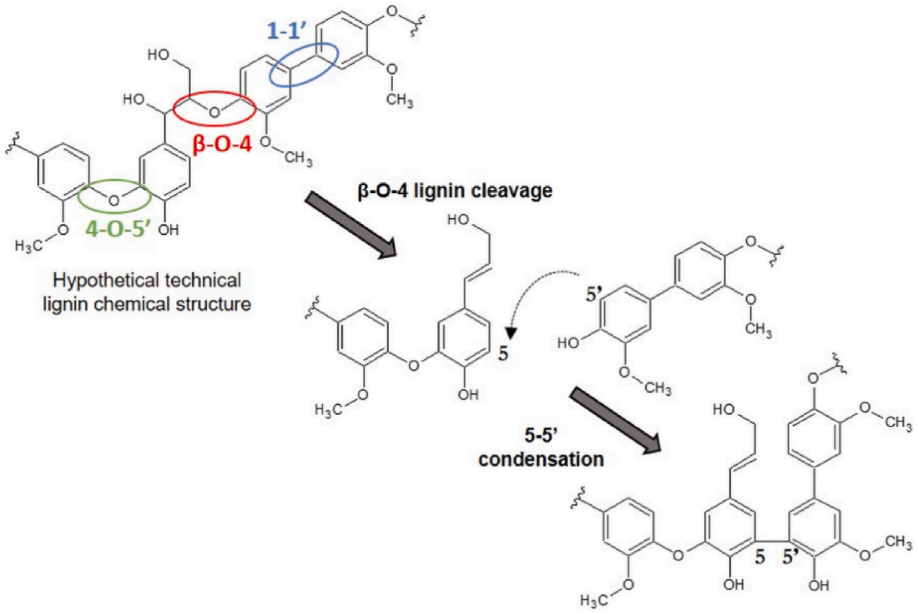

Fig. 5. Simplified reaction mechanism of the β-O-4 bond cleavage in lignin followed by the coupling reaction resulting 5-5′ interunit linkage in oligomeric structures.

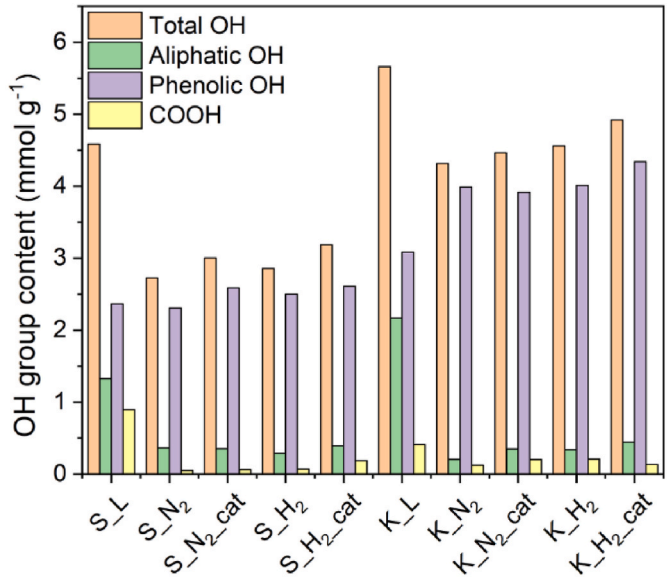

Fig. 6. The change of aliphatic and phenolic OH group content in lignins and oligomeric fragments (S_L- Soda lignin, S_*experimental conditions*- Soda oligomeric fragments after different reaction conditions, K_L- Kraft lignin, K_*experimental conditions*- Kraft oligomeric fragments after different reaction conditions.

for Soda (herbaceous) and Kraft (softwood) lignin are in accordance with literature [8,17,64,65]. The aliphatic OH group content in Soda oligomeric fragments significantly decreased and was determined to be 0.3 mmol g^{-1} and it becomes nearly unchanged for all oligomers at different reaction conditions. Furthermore, decarboxylation reactions importantly influenced total OH group content for Soda lignin with a noteworthy decrease of COOH groups in oligomers caused by hydrodeoxygenation, while minor effects of decarboxylation were observed for Kraft lignin. This confirms the efficiency of the lignin hydrodeoxygenation reactions and may explain the decrease in O/C ratio observed from elemental analysis (Fig. 2). The change in aliphatic and phenolic OH group content is observed for Kraft lignin and oligomeric fragments at different reaction conditions. The more prominent increase (compared to Soda lignin) in phenolic OH group content between the oligomeric fragments could be related to the cleavage of ether linkages [8]. In this study, these linkages are more pronounced in Kraft than Soda lignin. Thus, in addition to the emergence of the new guaiacyl OH groups after the cleavage of the β-ethers, overall phenolic OH group content also increases due to the appearance of C_5-substituted OH groups, as shown by the ^{31}P and 2D HSQC NMR spectra shown in Fig. 4 and Fig. S4, respectively.

Moreover, the increase of the phenolic OH group content in Kraft oligomers could be additionally assigned to the demethylation of the methoxy groups in G-units, which is also consistent with the reduced integral ratio between methoxy groups (CH_3O) and total aromatics (Ar) from 9.7 to 6.5 (Fig. 4). On the other hand, the phenolic OH group content was in range from 2.4 to 2.6 mmol g^{-1} with minor increase for Soda oligomers. In the case of Soda lignin, a comparable decrease of the CH_3O/Ar from 9.9 to 7.3 in combination with the relatively unchanged phenolic OH group content (Fig. 6) points towards the prevalence of demethoxylation reactions. Different Kraft (prevalence of demethylation) and Soda lignin (prevalence of demethoxylation) behavior under the same treatment conditions most likely is a result of the lignin structural differences, whereas the steric hindrance is one of the most important features [66]. There are studies reporting on the selectivity of the demeth (ox)ylation of the CH_3O group depending on the structural differences of the reactant, specifically the dominance of the demethylation and demethoxylation reactions was observed during the hydrodeoxygenation of guaiacol and 4-propylguaiacol, respectively [53,67]. Therefore, the structural differences such as the higher Mw of Kraft lignin (8600 Da) and the higher degree of condensation within G units could possibly determine the effects of the hydrodeoxygenation. Accordingly, lower Mw of the Soda lignin (4200 Da) and lower degree of the G unit condensation (S/G = 2.1) would possibly be a reason for the predominance of the demethoxylation reactions.

3.7. GC-MS analysis

Samples taken from the reaction mixture were analyzed using GC-MS. The yield of monomers was calculated using hexadecane as an internal standard [46]. The list of all quantified monomers and the yields of the quantified (selected) monomers are displayed in Table S7 and Fig. 7, respectively. Reproducibility of the experiments is presented in Fig. S5. The highest total amount of monomers produced after the catalytic Soda LD was 5.9 wt% and in case of Kraft lignin – 4.4 wt%.

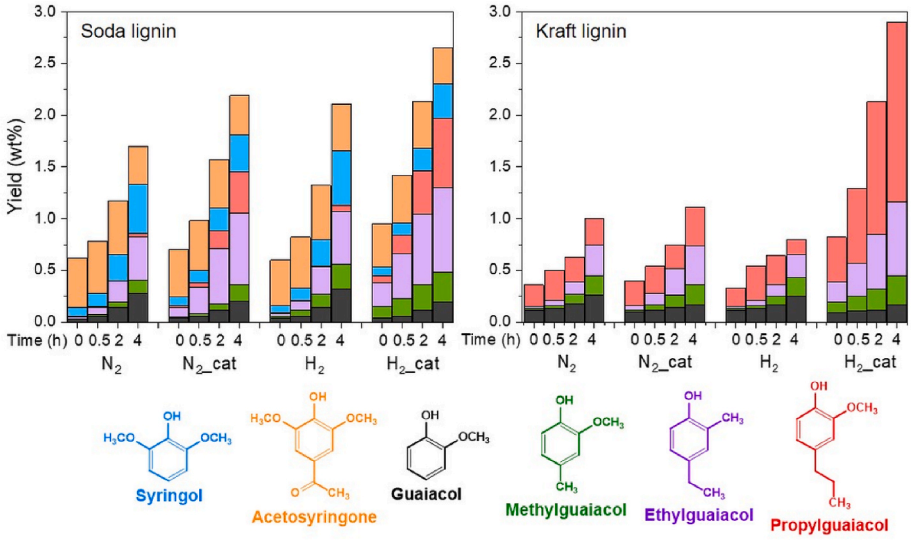

Fig. 7. The yield of monomers obtained after Soda and Kraft lignin depolymerization as a function of time.

Though, the yield of selected monomers (structurally simple syringyl and guaiacyl products) displayed in Fig. 7 is 2.7 wt% and 2.9 wt%, respectively. The continuous increase of the monomer yields was observed even during the non-catalytic depolymerization for both lignins. However, as it is evident from Fig. 7, the significant increase in monomers yields was obtained only for catalytic LD under reductive atmosphere.

Fig. 7 shows the yields of the main aromatic monomers obtained from Soda lignin. Here, guaiacol, methyl-, ethyl- and propylguaiacol were derived from the G-units or were possibly formed by demethoxylation of the present S-units [68,69], while syringol and acetosyringone were derived only from the S-units in Soda lignin. Acetosyringone is formed independently of the conditions in an earlier step of the reaction, and the yield is not significantly affected by the reactive conditions. Syringol, guaiacol, ethylguaiacol, methylguaiacol, and propylguaiacol are mainly formed after 2 h of reaction time. The highest yields of ethyl- and propylguaiacol were obtained at the end of the treatment. The most effective Soda LD was achieved using catalyst under the hydrogen atmosphere. However, the highest yields of guaiacol and syringol were obtained after the non-catalytic treatment at 0.3 wt% and 0.5 wt%, respectively. The high yield of propylguaiacol could be due to the stabilization of the propyl side chains by the Ru/C catalyst during Soda lignin depolymerization while ethylguaiacol and methylguaiacol are also subsequently formed by catalytic cracking of the lignin macromolecule [70].

The predominance of the G-units in the Kraft lignin structure accordingly determines the emergence of the guaiacyl products shown in Fig. 7. Hence, the highest yield of propylguaiacol up to 1.8 wt% was achieved using catalyst under the hydrogen atmosphere, while lower, but still noteworthy, yield of ethylguaiacol was up to 0.8 wt%. As it is evident from Fig. 7, only minor changes in guaiacol and methylguaiacol yields were detected within the 4-h reaction under the different conditions for Kraft lignin.

4. Discussion

The simplified lignin depolymerization mechanism is proposed to occur via cleavage of the β-O-4 bonds in technical lignins. Under supercritical conditions, quinone methide or aldehyde intermediates are formed, which are either stabilized by an H-donor atom or facilitate the formation of a solid residue. Upon successful cleavage of the β-O-4 bond and stabilization of the reactive radicals, smaller lignin-like oligomers are formed. Li et al. [71] reported that monomers are formed by the lignin end-unit rather than inter-unit, which was also supported by a kinetic study, suggesting that lignin monomers could be formed in parallel by the cleavage of the β-O-4 bond in the lignin or oligomeric fragment end-unit. On the other hand, the solid residue could be formed by condensation of remaining dimeric or oligomeric fragments or by two monomeric components with reactive OH groups and unsaturated side-chain carbons. The possible coupling mechanism of solid residue formation was in detail investigated by Huang et al. [40] and Ročnik Kozmelj et al. [53].

Soda (herbaceous) and Kraft (softwood) lignin depolymerization was evaluated using qualitative and (semi)quantitative analyses. The analyses were systematically used to upgrade lignin characterization with detailed insights into lignin chemistry and its behavior under inert and reductive atmosphere. The solid initial lignins and precipitated oligomers were analyzed by elemental analysis, GPC, UV-fluorescence and FTIR spectroscopy, and NMR (^{1}H-^{13}C HSQC and ^{31}P). In particular, GPC and NMR are comprehensive analytical techniques for the structural features of lignin that have been widely used for the interpretation of changes in lignin-like materials during the reaction process [8,17,43,64]. GPC analysis provides the size changes of the polymeric lignin macromolecule, while two different NMR methods allow detailed analysis of lignin functionality and prospects for the hydrotreatment process as the linkages in lignin are semi-quantified. Firstly, the elemental analysis was used to obtain H/C and O/C ratios in lignins and oligomers plotted in Van Krevelen diagrams (Fig. 2). The catalytic and non-catalytic process changed lignin functional groups and Mw which resulted in increased H/C ratio and decreased O/C ratio of oligomeric fragments. Additionally, GPC analysis of bio-oils and precipitated oligomers clearly emphasized that both lignins undergo depolymerization to form smaller fragments (oligomers) during liquefaction treatment, but the molecular weight of oligomers (about 1000 Da) is not highly affected by the catalysts nor the H_2. However, FTIR analysis of oligomers do not reveal important changes compare to initial lignin. Therefore, ^{31}P NMR and 2D HSQC analysis were employed to provide detailed structural features of lignin and oligomer samples. The emphasis was on the content of C-O and C-C bonds, appearance of the (condensed) guaiacyls and syringyls, and the change in the phenolic and aliphatic OH group content. Based on 2D HSQC NMR observations, precipitated oligomer chemical structures are significantly different from starting lignin. For both lignin catalytic reaction under reductive atmosphere improves the total conversion of ether bonds and aromatic units condensation. ^{31}P NMR showed, for both lignin, independently of reaction conditions, that aliphatic OH group and carboxylic group content are significantly

reduced compared to initial lignin. Concerning herbaceous Soda lignin, the total amount of phenolic OH group does not change significantly for all conditions whereas it notably changed for softwood Kraft lignin. It appears that the higher ether bonds content in starting Kraft lignin is the main explanation. The scission of ether bonds and 5-5′ condensation (Fig. 5) led to higher phenolic OH group content in Kraft oligomeric fragments.

Herbaceous sourced (Soda) lignin formed high amount of heavy aromatic components and fewer oligomeric fragments during non-catalytic LD. Contrary catalytic LD produced less SR and more oligomers. Thus, the Ru/C catalyst actively contributed to the stabilization of reactive radicals, H-transfer reactions and shifting to the formation of oligomers products in supercritical ethanol. UV fluorescence results confirmed that the catalyst actively stabilized reactive radicals with conversion to oligomeric and monomeric components under catalytic conditions. Additionally, the contribution of the reductive atmosphere is observable for more efficient conversion to monomers. Moreover, further analysis on the monomeric components by GC-MS confirmed that the presence of the Ru/C catalyst for Soda lignin is more important than reductive atmosphere. Indeed, the presence of reductive atmosphere slightly increases monomers yield from Soda lignin conversion whereas the presence of Ru/C catalyst outstandingly changes the yields and chemical composition of monomers. The catalytic conditions increase the monomer yield and promote the formation of alkylphenols (propylguaiacol and ethylguaiacol) potentially by the stabilization (hydrogenation) of species obtained after ether bonds rupture.

Softwood Kraft lignin consists mainly of guaiacyl units with an enhanced tendency to form solid recalcitrant products. It was also reported by Yong et al. [72] that guaiacyl units are the main constituents of solid residue. Similarly to herbaceous Soda lignin, the highest amount of SR was formed by non-catalytic reaction conditions, however with a noticeable difference in the amount of the hydrogenated oligomers with inert or reductive atmosphere. UV fluorescence results confirmed that the combination between catalyst and reductive atmosphere actively stabilized reactive radicals with conversion to oligomeric and monomeric components. Indeed, the combination of Ru/C catalyst and reductive significantly promote the formation of monomers (Fig. 7) for softwood Kraft lignin. In fact, compared to Soda lignin, the higher ether linkages content in Kraft lignin could explain this observation. The cleavage of weak linkages, such as β-O-4, produce free radicals or charged species which may form a new bond with another carbon atom (*e.g.* C=C) irreversibly leading to char-like structure [52]. Ru/C is described as an efficient catalyst for the hydrogenolysis of ether linkages especially with low hydrogen pressure [22]. The catalyst is described to ensure a rapid catalytic hydrogenation of reactive fragments prone to polymerization [73]. Consequently, in our study, due to the higher amount of intermediates emerging from the higher ether bonds content in Kraft lignin, the combination of external hydrogen source and active Ru/C catalyst is required to promote the stabilization of oligomeric and monomeric components while preventing repolymerization.

The results lead to the conclusion that a catalyst is absolutely required for technical lignin depolymerization. Therefore, the reuse of the catalyst is an important aspect that should be discussed and investigated in the future for potential pilot and/or industrial applications. Reusing the catalyst will contribute to a more sustainable and cost-efficient process, while reusability will provide valuable and useful methods for lignin depolymerization in the long term. However, the main challenge for reusability remains the separation of the catalyst from the solid residue.

5. Conclusion

The effect of the atmosphere (H_2/N_2) and the Ru-based catalyst was studied for the technical lignins depolymerization in supercritical ethanol in line with complementary analytical techniques to evaluate the chemistry of the reactions. The structural features of Soda and Kraft lignins were found to be significant parameters in explaining the distribution and yields of monomers, oligomers and solid residue. Larger amounts of solid residue and fewer oligomers were formed in the case of the Kraft lignin, composed mainly of guaiacyl units compared to Soda lignin containing both guaiacyl and syringyl units. Additionally, the reported results disclosed that the efficiency of the softwood Kraft lignin depolymerization strongly depends on the presence of the Ru/C catalyst and external hydrogen supply.

We have also provided important chemical characterization of the oligomers (^{31}P and 2D HSQC NMR) and proposed tentative chemical structure showing the absence of the cleavable ether bonds, while proposing the appearance of new 5-5′ bonds within phenolic inter-units. Additionally, the changes of aliphatic and aromatic OH group content propose the formation of more condensed oligomeric structures with reduced oxygen content and demeth (ox)ylation reactions, which are believed to depend on the structural features of lignin. The yields of S- and G-unit monomers are nicely correlated with the structure of the initial lignin.

CRediT authorship contribution statement

Tina Ročnik Kozmelj: Conceptualization, Formal analysis, Investigation, Writing – original draft, Visualization. **Erika Bartolomei:** Formal analysis, Investigation, Methodology. **Anthony Dufour:** Funding acquisition, Supervision. **Sebastien Leclerc:** Formal analysis, Investigation, Methodology. **Philippe Arnoux:** Formal analysis, Investigation, Methodology. **Blaž Likozar:** Funding acquisition, Supervision. **Edita Jasiukaitytė-Grojzdek:** Conceptualization, Supervision, Visualization, Writing – review & editing. **Miha Grilc:** Funding acquisition, Supervision, Writing – review & editing. **Yann Le Brech:** Conceptualization, Supervision, Writing – review & editing, Visualization.

Data availability

Data will be made available on request.

Funding and Acknowledgements

This research was funded by the Slovenian Research Agency (research core funding P2–0152 and research projects J2–2492, J2–1723 and L2-50050). This work was also supported by ANR (French National Research Agency) thought the project “Phenoliq”, Frederique Bertaud (CTP, Grenoble) is kindly acknowledged for providing softwood Kraft lignin. Isabelle Zigler (Université de Lorraine) is kindly acknowledged for her assistant into GPC analysis. Linda Bosser (Université de Lorraine) is kindly acknowledged for administrative management.

Appendix A. Supplementary data

Supplementary data to this article can be found online at https://doi.org/10.1016/j.biombioe.2024.107056.

References

[1] Y. Liao, S.F. Koelewijn, G. van den Bossche, J. van Aelst, S. van den Bosch, T. Renders, K. Navare, T. Nicolaï, K. van Aelst, M. Maesen, H. Matsushima, J. M. Thevelein, K. van Acker, B. Lagrain, D. Verboekend, B.F. Sels, A sustainable wood biorefinery for low-carbon footprint chemicals production, Science 367 (2020) 1385–1390, https://doi.org/10.1126/science.aau1567, 80.

[2] W. Schutyser, T. Renders, S. Van Den Bosch, S.F. Koelewijn, G.T. Beckham, B. F. Sels, Chemicals from lignin: an interplay of lignocellulose fractionation, depolymerisation, and upgrading, Chem. Soc. Rev. 47 (2018) 852–908, https://doi.org/10.1039/c7cs00566k.

[3] X. Zhen, H. Li, Z. Xu, Q. Wang, J. Xu, S. Zhu, Z. Wang, Z. Yuan, Demethylation, phenolation, and depolymerization of lignin for the synthesis of lignin-based epoxy resin via a one-pot strategy, Ind. Crops Prod. 173 (2021) 114135, https://doi.org/10.1016/j.indcrop.2021.114135.

[4] M.B. Figueirêdo, P.J. Deuss, R.H. Venderbosch, H.J. Heeres, Catalytic hydrotreatment of pyrolytic lignins from different sources to biobased chemicals:

identification of feed-product relations, Biomass Bioenergy 134 (2020), https://doi.org/10.1016/j.biombioe.2020.105484.
[5] J. Zakzeski, P.C.A. Bruijnincx, A.L. Jongerius, B.M. Weckhuysen, The catalytic valorization of lignin for the production of renewable chemicals, Chem. Rev. 110 (2010) 3552–3599, https://doi.org/10.1021/cr900354u.
[6] J. Lappalainen, D. Baudouin, U. Hornung, J. Schuler, K. Melin, S. Bjelić, F. Vogel, J. Konttinen, T. Joronen, Sub- and supercritical water liquefaction of kraft lignin and black liquor derived lignin, Energies 13 (2020), https://doi.org/10.3390/en13133309.
[7] L.T. Nguyen, D.-P. Phan, A. Sarwar, M.H. Tran, O.K. Lee, E.Y. Lee, Valorization of industrial lignin to value-added chemicals by chemical depolymerization and biological conversion, Ind. Crops Prod. 161 (2021) 113219, https://doi.org/10.1016/j.indcrop.2020.113219.
[8] C. Crestini, H. Lange, M. Sette, D.S. Argyropoulos, On the structure of softwood kraft lignin, Green Chem. 19 (2017) 4104–4121, https://doi.org/10.1039/C7GC01812F.
[9] J.V. Vermaas, M.F. Crowley, G.T. Beckham, Molecular lignin solubility and structure in organic solvents, ACS Sustain. Chem. Eng. 8 (2020) 17839–17850, https://doi.org/10.1021/acssuschemeng.0c07156.
[10] S. Sahoo, M.Ö. Seydibeyoğlu, A.K. Mohanty, M. Misra, Characterization of industrial lignins for their utilization in future value added applications, Biomass Bioenergy 35 (2011) 4230–4237, https://doi.org/10.1016/j.biombioe.2011.07.009.
[11] R. Chaudhary, P.L. Dhepe, Depolymerization of lignin using a solid base catalyst, Energy Fuel. 33 (2019) 4369–4377, https://doi.org/10.1021/acs.energyfuels.9b00621.
[12] R. Chaudhary, P.L. Dhepe, Solid base catalyzed depolymerization of lignin into low molecular weight products, Green Chem. 19 (2017) 778–788, https://doi.org/10.1039/c6gc02701f.
[13] T. Ročnik, B. Likozar, E. Jasiukaitytė-Grojzdek, M. Grilc, Catalytic lignin valorisation by depolymerisation, hydrogenation, demethylation and hydrodeoxygenation: mechanism, chemical reaction kinetics and transport phenomena, Chem. Eng. J. 448 (2022) 137309, https://doi.org/10.1016/j.cej.2022.137309.
[14] C.H. Zhou, X. Xia, C.X. Lin, D.S. Tong, J. Beltramini, Catalytic conversion of lignocellulosic biomass to fine chemicals and fuels, Chem. Soc. Rev. 40 (2011) 5588–5617, https://doi.org/10.1039/c1cs15124j.
[15] R.B. Santos, P.W. Hart, H. Jameel, H.-M. Chang, Important reactions of lignin, Bioresources 8 (2013) 1456–1477.
[16] C. Mattsson, S.I. Andersson, T. Belkheiri, L.E. Åmand, L. Olausson, L. Vamling, H. Theliander, Using 2D NMR to characterize the structure of the low and high molecular weight fractions of bio-oil obtained from LignoBoost^{TM} kraft lignin depolymerized in subcritical water, Biomass Bioenergy 95 (2016) 364–377, https://doi.org/10.1016/j.biombioe.2016.09.004.
[17] S. Constant, H.L.J. Wienk, A.E. Frissen, P. De Peinder, R. Boelens, D.S. Van Es, R.J. H. Grisel, B.M. Weckhuysen, W.J.J. Huijgen, R.J.A. Gosselink, P.C.A. Bruijnincx, New insights into the structure and composition of technical lignins: a comparative characterisation study, Green Chem. 18 (2016) 2651–2665, https://doi.org/10.1039/c5gc03043a.
[18] G. Hao, H. Liu, Z. Chang, K. Song, X. Yang, H. Ma, W. Wang, Catalytic depolymerization of the dealkaline lignin over Co–Mo–S catalysts in supercritical ethanol, Biomass Bioenergy 157 (2022) 106330, https://doi.org/10.1016/j.biombioe.2021.106330.
[19] S.O. Limarta, J.M. Ha, Y.K. Park, H. Lee, D.J. Suh, J. Jae, Efficient depolymerization of lignin in supercritical ethanol by a combination of metal and base catalysts, J. Ind. Eng. Chem. 57 (2018) 45–54, https://doi.org/10.1016/j.jiec.2017.08.006.
[20] J.Y. Kim, J. Park, U.J. Kim, J.W. Choi, Conversion of lignin to phenol-rich oil fraction under supercritical alcohols in the presence of metal catalysts, Energy Fuel. 29 (2015) 5154–5163, https://doi.org/10.1021/acs.energyfuels.5b01055.
[21] I. Hita, P.J. Deuss, G. Bonura, F. Frusteri, H.J. Heeres, Biobased chemicals from the catalytic depolymerization of Kraft lignin using supported noble metal-based catalysts, Fuel Process. Technol. 179 (2018) 143–153, https://doi.org/10.1016/j.fuproc.2018.06.018.
[22] M.A. Hossain, T.K. Phung, M.S. Rahaman, S. Tulaphol, J.B. Jasinski, N. Sathitsuksanoh, Catalytic cleavage of the B-O-4 aryl ether bonds of lignin model compounds by Ru/C catalyst, Appl. Catal. Gen. 582 (2019) 1–7, https://doi.org/10.1016/j.apcata.2019.05.034.
[23] S.O. Limarta, H. Kim, J.M. Ha, Y.K. Park, J. Jae, High-quality and phenolic monomer-rich bio-oil production from lignin in supercritical ethanol over synergistic Ru and Mg-Zr-oxide catalysts, Chem. Eng. J. 396 (2020) 125175, https://doi.org/10.1016/j.cej.2020.125175.
[24] I. Kristianto, S.O. Limarta, H. Lee, J.M. Ha, D.J. Suh, J. Jae, Effective depolymerization of concentrated acid hydrolysis lignin using a carbon-supported ruthenium catalyst in ethanol/formic acid media, Bioresour. Technol. 234 (2017) 424–431, https://doi.org/10.1016/j.biortech.2017.03.070.
[25] Y. Sang, H. Chen, M. Khalifeh, Y. Li, Catalysis and chemistry of lignin depolymerization in alcohol solvents - a review, Catal. Today 408 (2023) 168–181, https://doi.org/10.1016/j.cattod.2022.06.005.
[26] X. Huang, T.I. Korányi, M.D. Boot, E.J.M. Hensen, Ethanol as capping agent and formaldehyde scavenger for efficient depolymerization of lignin to aromatics, Green Chem. 17 (2015) 4941–4950, https://doi.org/10.1039/c5gc01120e.
[27] K. Cui, L. Yang, Z. Ma, F. Yan, K. Wu, Y. Sang, H. Chen, Y. Li, Selective conversion of guaiacol to substituted alkylphenols in supercritical ethanol over MoO3, Appl. Catal. B Environ. 219 (2017) 592–602, https://doi.org/10.1016/j.apcatb.2017.08.009.
[28] E. Roduner, Understanding catalysis, Chem. Soc. Rev. 43 (2014) 8226–8239, https://doi.org/10.1039/c4cs00210e.
[29] W. Cai, L. Li, R. Cao, S. Yang, H. Lu, Hydrodynamics of supercritical ethanol fluid-particles fluidization using low density ratio kinetic theory of granular flow, Chem. Eng. Sci. 260 (2022) 117926, https://doi.org/10.1016/j.ces.2022.117926.
[30] L. Cao, C. Zhang, H. Chen, D.C.W. Tsang, G. Luo, S. Zhang, J. Chen, Hydrothermal liquefaction of agricultural and forestry wastes: state-of-the-art review and future prospects, Bioresour. Technol. 245 (2017) 1184–1193, https://doi.org/10.1016/j.biortech.2017.08.196.
[31] H. Li, G. Song, Ru-catalyzed hydrogenolysis of lignin: base-dependent tunability of monomeric phenols and mechanistic study, ACS Catal. 9 (2019) 4054–4064, https://doi.org/10.1021/acscatal.9b00556.
[32] S. Wang, W.X. Li, Y.Q. Yang, X. Chen, J. Ma, C. Chen, L.P. Xiao, R.C. Sun, Unlocking structure–reactivity relationships for catalytic hydrogenolysis of lignin into phenolic monomers, ChemSusChem 13 (2020) 4548–4556, https://doi.org/10.1002/cssc.202000785.
[33] E. Bartolomei, Y. Le Brech, R. Gadiou, F. Bertaud, S. Leclerc, L. Vidal, J.M. Le Meins, A. Dufour, Depolymerization of technical lignins in supercritical ethanol: effects of lignin structure and catalyst, Energy Fuel. 35 (2021) 17769–17783, https://doi.org/10.1021/acs.energyfuels.1c02704.
[34] S. Lotfi, R. Mollaabbasi, G.S. Patience, Kinetics of softwood kraft lignin inert and oxidative thermolysis, Biomass Bioenergy 109 (2018) 239–248, https://doi.org/10.1016/j.biombioe.2017.11.011.
[35] H. Zhang, T. Chen, Y. Li, Y. Han, Y. Sun, G. Sun, Novel lignin-containing high-performance adhesive for extreme environment, Int. J. Biol. Macromol. 164 (2020) 1832–1839, https://doi.org/10.1016/j.ijbiomac.2020.07.307.
[36] C. Jiang, J. Hu, C. Zhang, G. Hota, J. Wang, N.G. Akhmedov, Lignin oligomers from mild base-catalyzed depolymerization for potential application in aqueous soy adhesive as phenolic blends, React. Chem. Eng. 8 (2023) 2455–2465, https://doi.org/10.1039/d3re00224a.
[37] I. Ullah, Z. Chen, Y. Xie, S.S. Khan, S. Singh, C. Yu, G. Cheng, Recent advances in biological activities of lignin and emerging biomedical applications: a short review, Int. J. Biol. Macromol. 208 (2022) 819–832, https://doi.org/10.1016/j.ijbiomac.2022.03.182.
[38] P. Figueiredo, K. Lintinen, J.T. Hirvonen, M.A. Kostiainen, H.A. Santos, Properties and chemical modifications of lignin: towards lignin-based nanomaterials for biomedical applications, Prog. Mater. Sci. 93 (2018) 233–269, https://doi.org/10.1016/j.pmatsci.2017.12.001.
[39] A. Boarino, J. Charmillot, M.B. Figueirêdo, T.T.H. Le, N. Carrara, H.-A. Klok, Ductile, high-lignin-content thermoset films and coatings, ACS Sustain. Chem. Eng. (2023), https://doi.org/10.1021/acssuschemeng.3c03030.
[40] X. Huang, T.I. Korányi, M.D. Boot, E.J.M. Hensen, Catalytic depolymerization of lignin in supercritical ethanol, ChemSusChem 7 (2014) 2276–2288, https://doi.org/10.1002/cssc.201402094.
[41] E. Bartolomei, Y. Le Brech, A. Dufour, V. Carre, F. Aubriet, E. Terrell, M. Garcia-Perez, P. Arnoux, Lignin depolymerization: a comparison of methods to analyze monomers and oligomers, ChemSusChem 13 (2020) 4633–4648, https://doi.org/10.1002/cssc.202001126.
[42] F. Tran, C.S. Lancefield, P.C.J. Kamer, T. Lebl, N.J. Westwood, Selective modification of the β–β linkage in DDQ-treated Kraft lignin analysed by 2D NMR spectroscopy, Green Chem. 17 (2015) 244–249, https://doi.org/10.1039/C4GC01012D.
[43] D.S. Zijlstra, A. De Santi, B. Oldenburger, J. De Vries, K. Barta, P.J. Deuss, Extraction of lignin with high β-O-4 content by mild ethanol extraction and its effect on the depolymerization yield, J. Vis. Exp. 2019 (2019), https://doi.org/10.3791/58575.
[44] X. Meng, C. Crestini, H. Ben, N. Hao, Y. Pu, A.J. Ragauskas, D.S. Argyropoulos, Determination of hydroxyl groups in biorefinery resources via quantitative 31P NMR spectroscopy, Nat. Protoc. 14 (2019) 2627–2647, https://doi.org/10.1038/s41596-019-0191-1.
[45] E. Jasiukaitytė-Grojzdek, M. Huš, M. Grilc, B. Likozar, Acid-catalyzed α-O-4 aryl-ether cleavage mechanisms in (aqueous) γ-valerolactone: catalytic depolymerization reactions of lignin model compound during organosolv pretreatment, ACS Sustain. Chem. Eng. 8 (2020) 17475–17486, https://doi.org/10.1021/acssuschemeng.0c06099.
[46] J.Y. De Saint Laumer, E. Cicchetti, P. Merle, J. Egger, A. Chaintreau, Quantification in gas chromatography: prediction of flame ionization detector response factors from combustion enthalpies and molecular structures, Anal. Chem. 82 (2010) 6457–6462, https://doi.org/10.1021/ac1006574.
[47] R. Olcese, V. Carré, F. Aubriet, A. Dufour, Selectivity of bio-oils catalytic hydrotreatment assessed by petroleomic and GC*GC/MS-FID analysis, Energy Fuel. 27 (2013) 2135–2145, https://doi.org/10.1021/ef302145g.
[48] W. Fang, M. Alekhina, O. Ershova, S. Heikkinen, H. Sixta, Purification and characterization of kraft lignin, Holzforschung 69 (2015) 943–950, https://doi.org/10.1515/hf-2014-0200.
[49] A. Agarwal, Y.-T. Jo, J.-H. Park, Hybrid microwave-ultrasound assisted catalyst-free depolymerization of Kraft lignin to bio-oil, Ind. Crops Prod. 162 (2021) 113300, https://doi.org/10.1016/j.indcrop.2021.113300.
[50] E. Jasiukaitytė-Grojzdek, M. Huš, M. Grilc, B. Likozar, Acid-catalysed α-O-4 aryl-ether bond cleavage in methanol/(aqueous) ethanol: understanding depolymerisation of a lignin model compound during organosolv pretreatment, Sci. Rep. 10 (2020), https://doi.org/10.1038/s41598-020-67787-9.
[51] L. Luo, J. Yang, G. Yao, F. Jin, Controlling the selectivity to chemicals from catalytic depolymerization of kraft lignin with in-situ H2, Bioresour. Technol. 264 (2018) 1–6, https://doi.org/10.1016/j.biortech.2018.03.062.

[52] E.I. Kozliak, A. Kubátová, A.A. Artemyeva, E. Nagel, C. Zhang, R.B. Rajappagowda, A.L. Smirnova, Thermal liquefaction of lignin to aromatics: efficiency, selectivity, and product analysis, ACS Sustain. Chem. Eng. 4 (2016) 5106–5122, https://doi.org/10.1021/acssuschemeng.6b01046.

[53] T. Ročnik Kozmelj, M. Žula, J. Teržan, B. Likozar, U. Maver, L. Činč Ćurić, E. Jasiukaitytė-Grojzdek, M. Grilc, Understanding stability, oligomerization and deactivation during catalytic lignin hydrodeoxygenation by mechanistic reaction micro-kinetics linked with 3D catalyst particle nanotomography, J. Clean. Prod. 414 (2023), https://doi.org/10.1016/j.jclepro.2023.137701.

[54] M. Verziu, A. Tirsoaga, B. Cojocaru, C. Bucur, B. Tudora, A. Richel, M. Aguedo, A. Samikannu, J.P. Mikkola, Hydrogenolysis of lignin over Ru-based catalysts: the role of the ruthenium in a lignin fragmentation process, Mol. Catal. 450 (2018) 65–76, https://doi.org/10.1016/j.mcat.2018.03.004.

[55] J. Long, Y. Xu, T. Wang, Z. Yuan, R. Shu, Q. Zhang, L. Ma, Efficient base-catalyzed decomposition and in situ hydrogenolysis process for lignin depolymerization and char elimination, Appl. Energy 141 (2015) 70–79, https://doi.org/10.1016/j.apenergy.2014.12.025.

[56] R. Rinaldi, R. Jastrzebski, M.T. Clough, J. Ralph, M. Kennema, P.C.A. Bruijnincx, B. M. Weckhuysen, Paving the way for lignin valorisation: recent advances in bioengineering, biorefining and catalysis, Angew. Chem., Int. Ed. 55 (2016) 8164–8215, https://doi.org/10.1002/anie.201510351.

[57] E. Terrell, M. Garcia-Perez, Novel strategy to analyze fourier transform ion cyclotron resonance mass spectrometry data of biomass pyrolysis oil for oligomeric structure assignment, Energy Fuel. 34 (2020) 8466–8481, https://doi.org/10.1021/acs.energyfuels.0c01687.

[58] R. Vendamme, J. Behaghel de Bueren, J. Gracia-Vitoria, F. Isnard, M.M. Mulunda, P. Ortiz, M. Wadekar, K. Vanbroekhoven, C. Wegmann, R. Buser, F. Héroguel, J. S. Luterbacher, W. Eevers, Aldehyde-assisted lignocellulose fractionation provides unique lignin oligomers for the design of tunable polyurethane bioresins, Biomacromolecules 21 (2020) 4135–4148, https://doi.org/10.1021/acs.biomac.0c00927.

[59] N. Giummarella, P.A. Lindén, D. Areskogh, M. Lawoko, Fractional profiling of kraft lignin structure: unravelling insights on lignin reaction mechanisms, ACS Sustain. Chem. Eng. 8 (2020) 1112–1120, https://doi.org/10.1021/acssuschemeng.9b06027.

[60] C.S. Lancefield, N.J. Westwood, The synthesis and analysis of advanced lignin model polymers, Green Chem. 17 (2015) 4980–4990, https://doi.org/10.1039/c5gc01334h.

[61] J. Gierer, Chemical aspects of kraft pulping, Wood Sci. Technol. 14 (1980) 241–266, https://doi.org/10.1007/BF00383453.

[62] A. Granata, D.S. Argyropoulos, 2-Chloro-4,4,5,5-tetramethyl-1,3,2-dioxaphospholane, a reagent for the accurate determination of the uncondensed and condensed phenolic moieties in lignins, J. Agric. Food Chem. 43 (1995) 1538–1544, https://doi.org/10.1021/jf00054a023.

[63] M. Balakshin, E. Capanema, On the quantification of lignin hydroxyl groups with 31P and 13C NMR spectroscopy, J. Wood Chem. Technol. 35 (2015) 220–237, https://doi.org/10.1080/02773813.2014.928328.

[64] P. Korntner, I. Sumerskii, M. Bacher, T. Rosenau, A. Potthast, Characterization of technical lignins by NMR spectroscopy: optimization of functional group analysis by 31P NMR spectroscopy, Holzforschung 69 (2015) 807–814, https://doi.org/10.1515/hf-2014-0281.

[65] R.J.A. Gosselink, J.E.G. van Dam, E. de Jong, E.L. Scott, J.P.M. Sanders, J. Li, G. Gellerstedt, Fractionation, analysis, and PCA modeling of properties of four technical lignins for prediction of their application potential in binders, Holzforschung 64 (2010), https://doi.org/10.1515/hf.2010.023.

[66] F.M. Harth, B. Hočevar, T.R. Kozmelj, E. Jasiukaitytė-Grojzdek, J. Blüm, M. Fiedel, B. Likozar, M. Grilc, Selective demethylation reactions of biomass-derived aromatic ether polymers for bio-based lignin chemicals, Green Chem. (2023), https://doi.org/10.1039/d3gc02867d.

[67] A.K. Deepa, P.L. Dhepe, Function of metals and supports on the hydrodeoxygenation of phenolic compounds, Chempluschem 79 (2014) 1573–1583, https://doi.org/10.1002/cplu.201402145.

[68] C.E.J.J. Vriamont, T. Chen, C. Romain, P. Corbett, P. Manageracharath, J. Peet, C. M. Conifer, J.P. Hallett, G.J.P. Britovsek, From lignin to chemicals: hydrogenation of lignin models and mechanistic insights into hydrodeoxygenation via low-temperature C-O bond cleavage, ACS Catal. 9 (2019) 2345–2354, https://doi.org/10.1021/acscatal.8b04714.

[69] B. Du, B. Liu, X. Wang, J. Zhou, A comparison of phenolic monomers produced from different types of lignin by phosphotungstic acid catalysts, ChemistryOpen 8 (2019) 643–649, https://doi.org/10.1002/open.201900088.

[70] P.T. Patil, U. Armbruster, M. Richter, A. Martin, Heterogeneously catalyzed hydroprocessing of organosolv lignin in sub- and supercritical solvents, Energy Fuel. 25 (2011) 4713–4722, https://doi.org/10.1021/ef2009875.

[71] Y. Li, B. Demir, L.M. Vázquez Ramos, M. Chen, J.A. Dumesic, J. Ralph, Kinetic and mechanistic insights into hydrogenolysis of lignin to monomers in a continuous flow reactor, Green Chem. 21 (2019) 3561–3572, https://doi.org/10.1039/c9gc00986h.

[72] T.L.K. Yong, Y. Matsumura, Reaction kinetics of the lignin conversion in supercritical water, Ind. Eng. Chem. Res. 51 (2012) 11975–11988, https://doi.org/10.1021/ie300921d.

[73] A. Kloekhorst, Y. Shen, Y. Yie, M. Fang, H.J. Heeres, Catalytic hydrodeoxygenation and hydrocracking of Alcell® lignin in alcohol/formic acid mixtures using a Ru/C catalyst, Biomass Bioenergy 80 (2015) 147–161, https://doi.org/10.1016/j.biombioe.2015.04.039.